Article ID: 1000-324X(2022)08-0911-07 **DOI:** 10.15541/jim20220025

Fabrication and Characterizations of Red Ce-doped 8YSZ Transparent Ceramics by Two-step Sintering

LIU Qiang[1], WANG Qian[1,2], CHEN Penghui[2,3], LI Xiaoying[2,3], ZHANG Lixuan[2,3], XIE Tengfei[2,3], LI Jiang[2,3]

(1. School of Material Science and Engineering, Jiangsu University, Zhenjiang 212013, China; 2. Key Laboratory of Transparent Opto-Functional Inorganic Materials, Shanghai Institute of Ceramics, Chinese Academy of Sciences, Shanghai 201899, China; 3. Center of Materials Science and Optoelectronics Engineering, University of Chinese Academy of Sciences, Beijing 100049, China)

Abstract: Color zirconia ceramics are widely used in electronics and decoration fields due to their bright colors, high refractive index, wear resistance, corrosion resistance, and non-toxicity to the human body. Cubic cerium doped 8% yttria mol percent stabilized zirconia (Ce-doped 8YSZ) nano-powder with average particle size of 15.9 nm was synthesized by co-precipitation method. Using the powder calcined at 800 ℃ for 4 h as starting material, red zirconia transparent ceramics with high optical transparency and high redness value were prepared by two-step sintering method. Influences of pre-sintering temperature on microstructure, in-line transmittance and color performance of the red Ce-doped 8YSZ ceramics were studied. As the pre-sintering temperature increases from 1200 ℃ to 1300 ℃, average grain size of the ceramics increases from 0.3 μm to 2.2 μm and the relative density increases from 87.2% to 97.1%. The Ce-doped 8YSZ ceramics pre-sintered at 1275 ℃ for 2 h and hot isostatic pressed (HIP) at 1700 ℃ for 3 h show the best in-line transmittance of 47.6% at 700 nm and the highest redness of 52.0.

Key words: Ce-doped 8YSZ; red transparent ceramics; air pre-sintering; hot isostatic pressing; optical property

In recent decades, the applications of zirconia material extend to dental restoration materials, smart terminal materials, color decoration materials and other potential fields[1-4], which is attributed to its outstanding mechanical properties, chemical inertness, optical properties and biocompatibility[5-7]. In the past, the cubic yttria stabilized zirconia single crystal is an interesting material for an application as diamond imitation because of its high refractive index of 2.2 and high hardness[8-12]. However, there are some drawbacks for the single crystals, such as high fabrication temperature (2750 °C), shape limitation and high cost[13]. In addition, the melting point of the colorants are much lower than that of the zirconia single crystal, causing serious volatilization of the coloring ions and making it difficult to achieve the desired colors. Investigations have demonstrated that zirconia transparent ceramics have many advantages compared with the zirconia single crystals[14-16]. For example, the preparation temperature of zirconia ceramics is low, which can avoid the volatilization of colorants.

In 1986, the first report on transparent c-ZrO_2 ceramics was published by Tsukuma[14]. Since then, polycrystalline c-ZrO_2 transparent ceramics have been widely investigated[15-18]. On one hand, c-ZrO_2 transparent ceramics were fabricated using commercially available yttria stabilized zirconia powders as starting materials. Peuchert, *et al.*[16] fabricated polycrystalline c-ZrO_2 transparent ceramics after sintering at 1650 ℃ for 3 h followed by HIP treatment at 1750 ℃ for 1 h using high purity cubic yttria stabilized zirconia powder (Tosoh Corporation, Tokyo, Japan), and the in-line transmittance of 5.6 mm thick samples reached 68% at 600 nm. On the other hand, co-precipitation method is an effective route to synthesize yttria stabilized zirconia nano-powders with good dispersity and high sinterability[17-18], and it is also widely used to prepare various transparent ceramics[19-21] because of its simple and economical process. Chen, *et al.*[22] prepared yttria-stabilized zirconia transparent ceramics

Received date: 2022-01-17; **Revised date:** 2022-03-17; **Published online:** 2022-04-07
Foundation item: National Key R&D Program of China (2021YFE0104800); Key Research Project of the Frontier Science of the Chinese Academy of Sciences (QYZDB-SSW-JSC022)
Biography: LIU Qiang (1964–), male, professor. E-mail: lq88611338@163.com
刘 强(1964–), 男, 教授. E-mail: lq88611338@163.com
Corresponding author: LI Jiang, professor. E-mail: lijiang@mail.sic.ac.cn
李 江, 研究员. E-mail: lijiang@mail.sic.ac.cn

after sintering at 1350 ℃ for 2 h and HIP treatment at 1800 ℃ for 3 h from the co-precipitated nano-powder, and the in-line transmittance of the ceramics with the thickness of 1.0 mm was 67.8% at 800 nm. Currently, there are also some investigations on zirconia ceramics with various colors[2,23].

By doping transition metals or rare earths, various colors can be observed in zirconia ceramics. Compared with other rare earth ions that exist mostly in a trivalent state, cerium exists in the form of Ce^{3+} and Ce^{4+} in the zirconia. Ce^{3+} can exhibits a strong absorption band at about 400 nm caused by 4f-5d transition, while Ce^{4+} does not show any absorption band in the visible range[24]. In order to obtain a red zirconia ceramic with high redness value, Lv *et al.* [25] fabricated Ce-doped red zirconia ceramics by a high-temperature reduction method, and the absorption band was in the range from 480 to 500 nm and the maximum redness value of the ceramics was 32. Additionally, iron oxide was widely used as a red colorant for the preparation of red ceramics[26-29]. Results showed that Fe_2O_3 had poor color rendering and the samples were orange-red. At present, the redness value of zirconia ceramics was low and few studies were conducted on transparent zirconia ceramics with red color which can broaden the application of zirconia ceramics in filters, signal lampshades and other fields.

In order to obtain red zirconia ceramics with high transparency and large redness value, two-step sintering method was used. In this work, the Ce-doped 8YSZ nano-powder used as the starting material was synthesized by a reverse co-precipitation method. Red Ce-doped 8YSZ transparent ceramics were prepared by air pre-sintering combined with HIP post-treatment. The influences of pre-sintering temperatures on microstructure, in-line transmittance and color parameters of Ce-doped 8YSZ ceramics were studied.

1 Experimental

$ZrOCl_2·8H_2O$ (99.5%, Zhongkai New Materials Co., Ltd., Jining, China) was dissolved in deionized water to obtain the solution containing Zr^{4+}. $Ce(NO_3)_3$ and $Y(NO_3)_3$ solutions were prepared by dissolving CeO_2 (99.995%, Golden Dragon Rare-earth Co., Ltd., Fujian, China) and Y_2O_3 (99.999%, Golden Dragon Rare-earth Co., Ltd., Fujian, China) into the high-purity hot nitric acid. The solutions were mixed in stoichiometrical proportions of Ce^{3+}:Zr^{4+}:Y^{3+}=0.01:0.91:0.16. Ammonium hydroxide (25.0%–28.0%, Sinopharm Chemical Reagent Co., Ltd., Shanghai, China) solution was used as precipitant solution and PEG4000 (Aladdin Industrial Co., Ltd., Shanghai, China) was added as dispersant. The mixed salt solution was dropped into the precipitant solution at a rate of 20 mL/min under stirring and the terminal pH was 9.0. After aging for 1 h at room temperature, the resultant slurry was washed for 4 times with deionized water and twice with anhydrous ethanol. After drying at 70 ℃ for 30 h, the precursor was seived through a 75 μm (200-mesh) screen. Then the precursor was calcined at 800 ℃ for 4 h to obtain the Ce-doped 8YSZ powder. After that, the powder was uniaxially dry-pressed into pellets at 40 MPa, and then cold isostatically pressed at 250 MPa to get the ceramic green bodies. The green pellets were pre-sintered at 1200–1300 ℃ for 2 h in air and HIP treated at 1700 ℃ for 3 h under 176 MPa in Ar atmosphere. The ceramic samples were then polished to 1 mm thickness for subsequent testing. The pre-sintered and HIP post-treated ceramics were thermally etched at 1100 and 1450 ℃ for 3 h, respectively.

Thermogravimetry and differential thermal analysis (TG-DTA, Thermo Plus Evo II, Rigaku, Japan) were used to test the thermal behavior of precursor in air at a heating rate of 10 ℃/min. X-ray diffraction (XRD, Model D/MAX2200 PC, Rigaku, Japan) was used to analyze the phase of the nano-powder and the ceramics in the range of 2θ=20°–80°, which was excited by a Cu K_α radiation. Norcross ASAP 2010 micromeritics was used to determine the specific surface area of the nano-powder with the nitrogen adsorption isothermal at 77 K. Field emission scanning electron microscope (FESEM, SU9000, Hitachi, Japan) was used to analyze the morphologies of precursor and calcined powder. The microstructures and energy-dispersive X-ray spectrometry (EDS) mapping of sintered ceramics were observed by field emission scanning electron microscope (FESEM, SU8220, Hitachi, Japan). UV-VIS-NIR spectrophotometer (Model Cary-5000, Varian, USA) was used to measure the in-line transmittance, absorption spectrum and the CIE value with the Color software. The $L^*\times a^*\times b^*$ colorimetry method recommended by the International Commission on Illumination (CIE 15-2004) was used. And the normal/normal geometry (0°:0°) for transmission measurements was used. For the color measurement system, L^* is the lightness axis 0 (black) – 100 (white), a^* is the red (+) – green (–) axis, and b^* is the yellow (+) – blue (–) axis.

2 Results and discussion

The TG-DTA curves of the Ce-doped 8YSZ precursor are shown in Fig. 1. The total weight loss of the precursor is 30.0% in the heating process from room temperature to 1200 ℃. The weight loss of 24.4% below

280 ℃ is mainly caused by the removal of absorbed water, hydrate water and residual ethanol and the decomposition of hydroxides, accompanied with a large endothermic peak at 115 ℃[19]. The exothermic peak at 290 ℃ is due to the decomposition of PEG4000. The exothermic peak at 461 ℃ is related to the crystallization of Ce-doped 8YSZ phase[30].

Fig. 2 shows the XRD patterns of the as-synthesized Ce-doped 8YSZ precursor and the powder calcined at 800 ℃ for 4 h. The result shows that the precursor is amorphous. After calcined at 800 ℃, the specimen shows good crystallinity and the peaks are consistent with the c-ZrO_2 phase (JCPDS 49-1642). The average crystallite size (D_{XRD}) of the Ce-doped 8YSZ powder is 11.5 nm calculated by Scherrer's formula using the full width at half maximum (FWHM) of XRD pattern.

Fig. 3 shows the FESEM micrographs of the Ce-doped 8YSZ precursor and the powder calcined at 800 ℃ for 4 h. It can be seen from Fig. 3(a) that the precursor is heavily aggregated. The reason for the agglomeration is the hydrogen bond between the hydroxides and the dispersant (PEG4000) covered on the surface of the precursor[17]. The powder exhibits good homogeneity and dispersity after calcination and the shape of the powder is quasi-spherical. The specific surface area (S_{BET}) of the

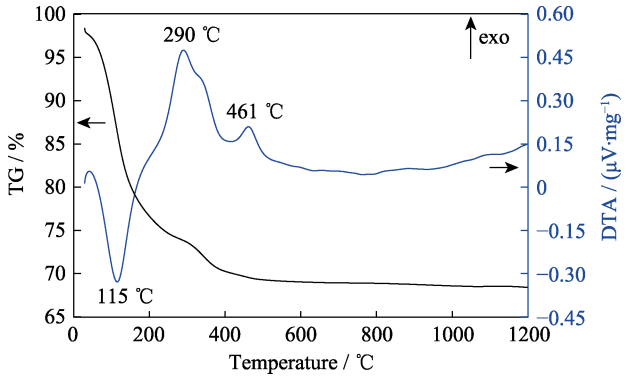

Fig. 1　TG-DTA curves of the Ce-doped 8YSZ precursor

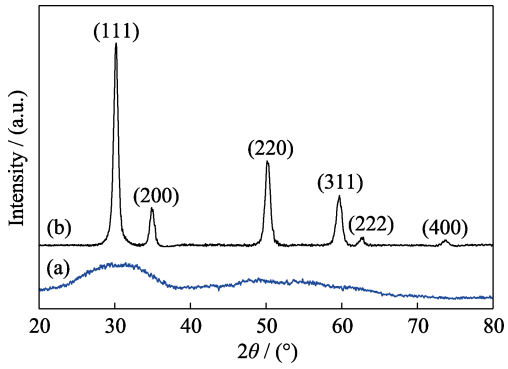

Fig. 2　XRD patterns of (a) Ce-doped 8YSZ precursor and (b) the powder calcined at 800 ℃ for 4 h

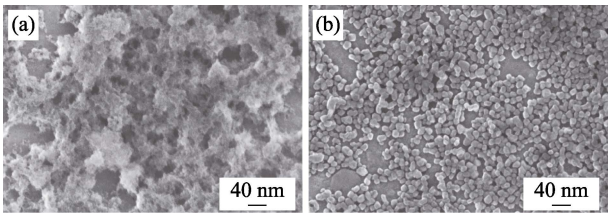

Fig. 3　FESEM micrographs of (a) Ce-doped 8YSZ precursor and (b) the powder calcined at 800 ℃ for 4 h

Ce-doped 8YSZ powder is 63.3 m^2/g and the average particle size (D_{BET}) is 15.9 nm.

Fig. 4 shows the FESEM micrographs of the thermally etched surfaces of Ce-doped 8YSZ ceramics pre-sintered at different temperatures in air for 2 h. The relative densities and the average grain size of corresponding ceramics are show in Fig. 5. It is noted that quite a few connected pores are located at the grain boundary of the ceramics sintered at 1200 ℃. The relative density of the ceramics is 87.2% and the average grain size is 0.3 μm. With the increase of pre-sintering temperature, the pores of the ceramics are gradually removed and the grain size gradually increases. As the sintering temperature increases to 1275 ℃, the residual pores are largely eliminated and the connected pores are transformed into isolated pores. Meanwhile, the relative density increases to 95.7%, and the average grain size increases to 1.1 μm. When the temperature further increases to 1300 ℃, some intragranular pores emerge, which are difficult to be removed by HIP post-treatment. The reason for this phenomenon is that

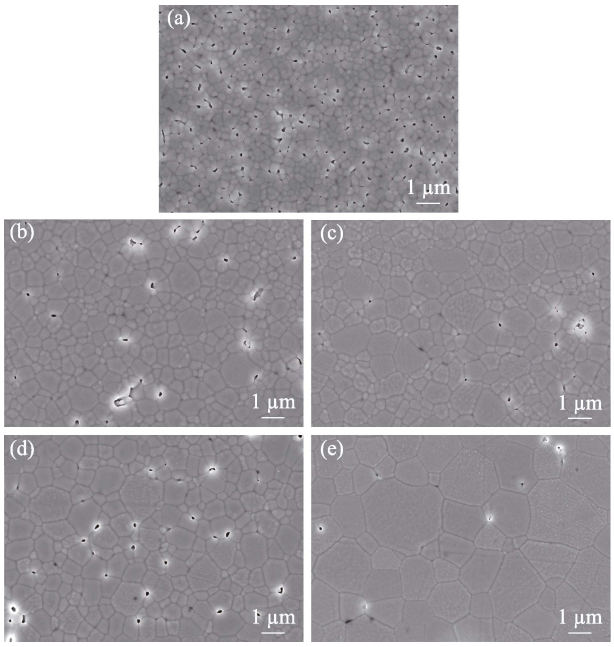

Fig. 4　FESEM micrographs of the thermally etched surfaces of Ce-doped 8YSZ ceramics pre-sintered at different temperatures in air for 2 h
(a) 1200 ℃; (b) 1230 ℃; (c) 1250 ℃; (d) 1275 ℃; (e) 1300 ℃

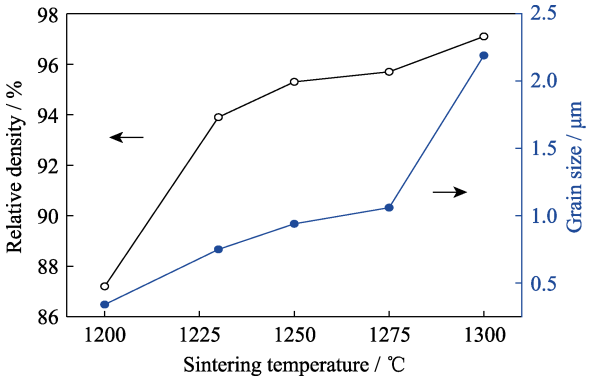

Fig. 5 Relative densities and average grain size of the Ce-doped 8YSZ ceramics pre-sintered at 1200–1300 ℃ in air for 2 h

the rate of grain boundary migration is faster than the rate of pores removal during the sintering process[31]. The average grain size and relative density rapidly increase to 2.2 μm and 97.1%, respectively, when the pre-sintering temperature reaches 1300 ℃.

Fig. 6(a-e) show the FESEM micrographs of the thermally etched surfaces of Ce-doped 8YSZ ceramics pre-sintered at 1200–1300 ℃ in air for 2 h combined with HIP post-treatment at 1700 ℃ for 3 h. It can be seen that the grain size and porosity of the ceramics after HIP post-treatment have changed significantly compared with the pre-sintered ceramics. The average grain size of the ceramics pre-sintered at 1200 ℃ increases to 4.7 μm after HIP treatment. The relative density of the ceramics only increases to 91.3%, and it can be noticed from Fig. 6(a) that there are still a lot of pores in the ceramics after HIP post-treatment. The reason for this phenomenon is that there are many open pores in the pre-sintered ceramics, which result in the infiltration of argon and elimination of the driving force of pore migration[32]. For the ceramics pre-sintered at 1230 and 1250 ℃ combined with HIP post treated at 1700 ℃, most of the pores are eliminated and the average grain sizes are 83 and 104 μm, respectively. Meanwhile some intragranular pores are formed because the migration rate of grain boundaries is faster than the remove rate of pores during the HIP post-treatment[31]. After HIP treatment, the ceramics pre-sintered at 1275 ℃ have a nearly pore-free microstructure due to the effective removal of intergranular pores and the average gain size is 110 μm. For the HIP-treated ceramics pre-sintered at 1300 ℃, the intragranular pores are still in the ceramics after HIP post-treatment. Fig. 6(f-i) show the EDS elemental mapping of the Ce-doped 8YSZ ceramics. The doped element of Ce is homogeneously distributed in the grains of the ceramics.

Fig. 7 shows the XRD patterns of the pre-sintered and

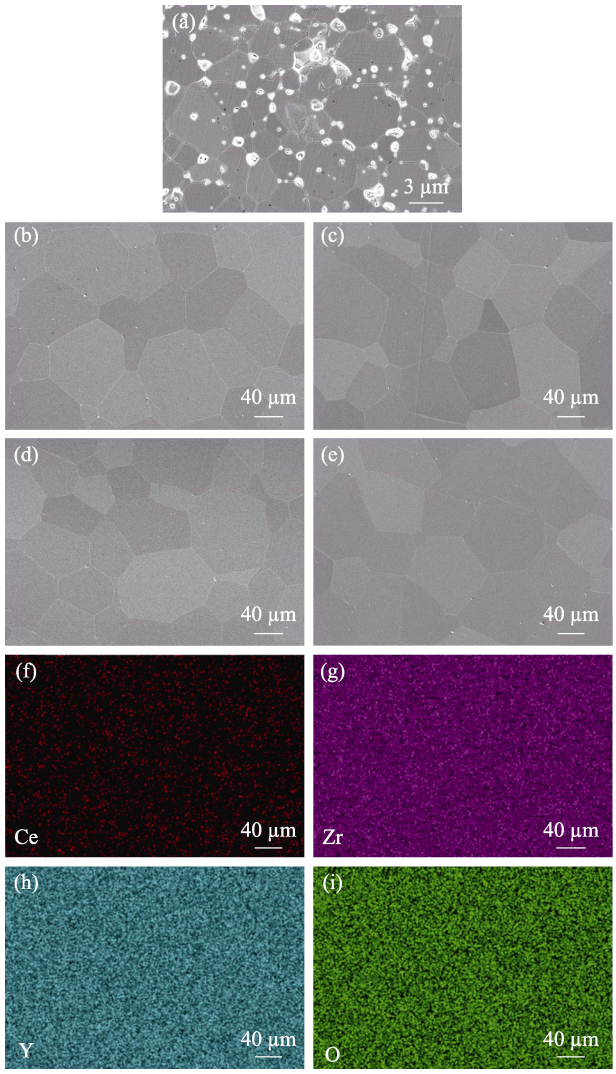

Fig. 6 (a-e) FESEM micrographs of the thermally etched surfaces of Ce-doped 8YSZ ceramics pre-sintered at 1200–1300 ℃ for 2 h and HIP post-treatment at 1700 ℃ for 3 h; (f-i) EDS element mapping of the Ce-doped 8YSZ ceramics pre-sintered at 1275 ℃

(a) 1200 ℃; (b) 1230 ℃; (c) 1250 ℃; (d) 1275 ℃; (e) 1300 ℃

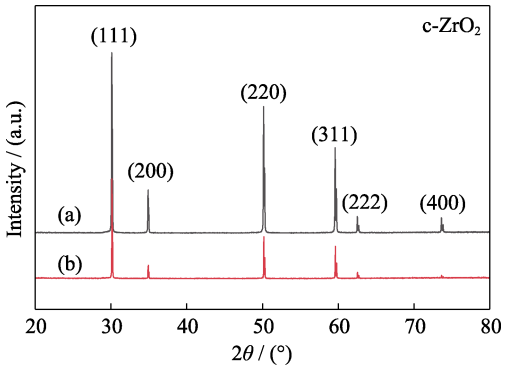

Fig. 7 XRD patterns of the (a) pre-sintering and (b) HIP-treatment ceramics

the HIP post-treated ceramics. The splitting peaks at high angles are caused by CuKα_2. The result shows that the

crystal structures of the ceramics before and after HIP treatment are both cubic fluorite type, which does not exhibit the birefringence effect at the grain boundaries.

Fig. 8 shows the photograph and the in-line transmittance of the Ce-doped 8YSZ ceramics with 1 mm thickness. It can be seen that the ceramics show a bright red due to the absorption of trivalent cerium that forms during the HIP post-treatment[24-25]. The in-line transmittance is nearly zero in the visible light range below 550 nm, and the light between 550 and 780 nm can pass through the ceramics[29]. The pre-sintering temperature has a great effect on the optical quality of ceramics. The ceramics pre-sintered at 1200 ℃ are opaque after the HIP post-treatment, and the result corresponds to the microstructure as shown in Fig. 6(a). The ceramics are transparent after pre-sintering at 1230–1300 ℃ and HIP post-treating at 1700 ℃, and the words in the picture can be clearly seen through the ceramics. With the increase of the pre-sintering temperature, the in-line transmittance of the ceramics firstly increases and then decreases. After HIP treatment, the ceramics pre-sintered at 1275 ℃ have the highest transparency and the in-line transmittance of Ce-doped 8YSZ ceramics is 47.6% at 700 nm. When the sintering temperature increases to 1300 ℃, the in-line transmittance of the ceramics decreases after HIP treatment due to the existence of intragranular pores formed during the pre-sintering. It can be seen in Fig. 8(b) that the in-line transmittance of the ceramics decreases with the decrease of the wavelength which is mainly due to the scattering center in the ceramics[32].

Fig. 9 shows the absorption spectra of the ceramics pre-sintered at different temperatures and HIP post-treated at 1700 ℃. The Ce-doped 8YSZ ceramics show a broad

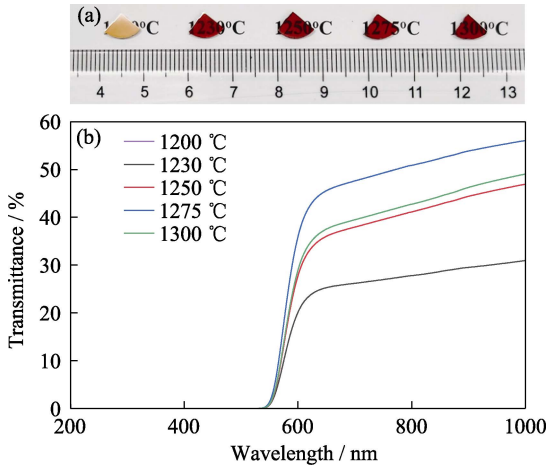

Fig. 8　(a) Photograph and (b) in-line transmittance of the Ce-doped 8YSZ ceramics (1 mm thick) pre-sintered at 1200–1300 ℃ in air for 2 h and HIP post-treatment at 1700 ℃ for 3 h under 176 MPa in Ar atmosphere

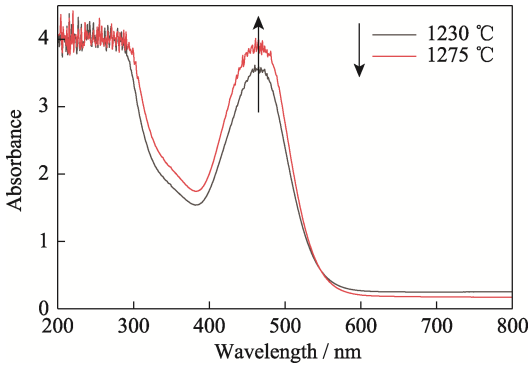

Fig. 9　Absorption spectra of the ceramics pre-sintered at different temperatures and HIP post-treatment at 1700 ℃

Table 1　CIE value of Ce-doped 8YSZ ceramics pre-sintered at 1230–1300 ℃ for 2 h and HIP post-treatment at 1700 ℃ for 3 h

Pre-sintering temperature/℃	Value of CIE		
	L^*	a^*	b^*
1230	31.8	42.5	54.7
1250	37.4	48.6	64.3
1275	42.4	52.0	72.9
1300	37.7	48.9	64.8

and strong absorption band in the visible light range within 400–550 nm, corresponding to the 4f-5d transition of Ce^{3+}, so the ceramics is red[33]. Table 1 shows the CIE value ($L^*\times a^*\times b^*$) of Ce-doped 8YSZ ceramics. It can be seen that the ceramics have high redness values, and the maximum redness value is 52.0. With the increase of the pre-sintering temperature, the color parameters of the ceramics firstly increase and then decrease. Compared with the ceramics pre-sintered at 1230 ℃, the ceramic samples pre-sintered at 1275 ℃ shows stronger absorption for blue-violet light around 400–500 nm and less absorption for orange-red light around 600–780 nm, so their $L^*\times a^*\times b^*$ values are larger, and the lightness value L^*, redness value a^* and yellowness value b^* of the ceramics are 42.4, 52.0 and 72.9, respectively.

3　Conclusions

In this work, Ce-doped 8YSZ transparent ceramics were prepared by air pre-sintering at 1200–1300 ℃ for 2 h combined with HIP post-treatment at 1700 ℃ for 3 h using the nano-powder synthesized *via* a co-precipitation method. By doping with cerium ions, the 8YSZ ceramics show a bright red color. The pre-sintering temperatures have a great influence on microstructure and optical performance. The ceramics pre-sintered at 1275 ℃ for 2 h combined with HIP post-treatment at 1700 ℃ for 3 h show the highest in-line transmittance of 47.6% at

700 nm and the biggest redness value of 52.0. The preparation temperature of zirconia ceramics is lower than the single crystals, which can effectively avoid the volatilization of colorants. Red Ce-doped 8YSZ transparent ceramics have wide application prospects in filter materials, signal lamp materials and other fields.

References:

[1] ZHANG X X, ZHU D B, LIANG J S. Progress on hydrothermal stability of dental zirconia ceramics. *J. Inorg. Mater.*, 2020, **35(7):** 759–768.

[2] LV H D, BAO J X, RUAN F, *et al*. Preparation and properties of black Ti-doped zirconia ceramics. *J. Mater. Res. Technol.*, 2020, **9(3):** 6201–6208.

[3] SANI E, SCITI D, CAPIANI C, *et al*. Colored zirconia with high absorbance and solar selectivity. *Scr. Mater.*, 2020, **186:** 147–151.

[4] LAGANOVSKA K, OLSTEINS D, SMITS K, *et al*. Formation of translucent nanostructured zirconia ceramics. *J. Eur. Ceram. Soc.*, 2021, **41(13):** 6641–6648.

[5] LEI L W, FU Z Y, WANG H, *et al*. Transparent yttria stabilized zirconia from glycine-nitrate process by spark plasma sintering. *Ceram. Int.*, 2012, **38(1):** 23–28.

[6] IKESUE A. Processing of ceramics: breakthroughs in optical materials. Hoboken: John Wiley and Sons, 2021**:** 275–348.

[7] BEJUGAMA S, CHAMEETTACHAL S, PATI F, *et al*. *In vitro* cellular response and hydrothermal aging of two-step sintered Nb_2O_5 doped ceria stabilized zirconia ceramics. *Ceram. Int.*, 2021, **47(2):** 1594–1601.

[8] WOOD D L, NASSAU K. Refractive index of cubic zirconia stabilized with yttria. *Appl. Opt.*, 1982, **21(16):** 2978–2981.

[9] TIAN T, XU J Y, ZHAN Z G, *et al*. Study on the spectral characteristics of emerald-like cubic zirconia crystal. *J. Synth. Cryst.*, 2015, **44(3):** 581–586.

[10] DASHA A, KIMB B N, KLIMKEC J, *et al*. Transparent tetragonal-cubic zirconia composite ceramics densified by spark plasma sintering and hot isostatic pressing. *J. Eur. Ceram. Soc.*, 2019, **39(4):** 1428–1435.

[11] ZHANG H B, KIM B N, MORITA K, *et al*. Optimization of high-pressure sintering of transparent zirconia with nano-sized grains. *J. Alloys Compd.*, 2010, **508(1):** 196–199.

[12] ZHANG H B, KIM B N, MORITA K, *et al*. Optical properties and microstructure of nanocrystalline cubic zirconia prepared by high-pressure spark plasma sintering. *J. Am. Ceram. Soc.*, 2011, **94(9):** 2981–2986.

[13] TIAN F, CHEN C, LIU Y, *et al*. Fabrication of Nd:YAG transparent ceramics from co-precipitated powders by vacuum pre-sintering and HIP post-treatment. *Opt. Mater.*, 2020, **101:** 109728.

[14] TSUKUMA K. Transparent titania-yttria-zirconia ceramics. *J. Mater. Sci. Lett.*, 1986, **5:** 1143–1144.

[15] TSUKUMA K, YAMASHITA I, KUSUNOSE T. Transparent 8mol% Y_2O_3-ZrO_2 (8Y) ceramics. *J. Am. Ceram. Soc.*, 2010, **91(3):** 813–818.

[16] PEUCHERT U, OKANO Y, MENKE Y, *et al*. Transparent cubic-ZrO_2 ceramics for application as optical lenses. *J. Eur. Ceram. Soc.*, 2009, **29(2):** 283–291.

[17] LIU Q, CHEN P H, JIANG N, *et al*. Fabrication and characterizations of 8.7mol% Y_2O_3-ZrO_2 transparent ceramics using co-precipitated nanopowders. *Scr. Mater.*, 2019, **171:** 98–101.

[18] LUO J M, CAO Z C, DENG L P, *et al*. Preparation and luminescence property of Ho^{3+}/Yb^{3+}:8YSZ nanopowders. *J. Synth. Cryst.*, 2017, **46(10):** 1902–1906.

[19] HUANG X Y, LIU Y M, LIU Y, *et al*. Fabrication and characterizations of Yb:YAG transparent ceramics using alcohol-water co-precipitation method. *J. Inorg. Mater.*, 2021, **36(2):** 217–224.

[20] LI X Y, SNETKOV I L, YAKOVLEV A, *et al*. Fabrication and performance evaluation of novel transparent ceramics RE:$Tb_3Ga_5O_{12}$ (RE=Pr, Tm, Dy) toward magneto-optical application. *J. Adv. Ceram.*, 2021, **10(2):** 271–278.

[21] LIU Z Y, TOCI G, PIRRI A, *et al*. Fabrication, microstructures, and optical properties of Yb:Lu_2O_3 laser ceramics from co-precipitated nano-powders. *J. Adv. Ceram.*, 2020, **9(6):** 674–682.

[22] CHEN P H, LIU Q, LI X Y, *et al*. Influence of terminal pH value on co-precipitated nanopowders for yttria-stabilized ZrO_2 transparent ceramics. *Opt. Mater.*, 2019, **98:** 109475.

[23] LV H D, BAO J X, QI S Y, *et al*. Optical and mechanical properties of purple zirconia ceramics. *J. Asian Ceram. Soc.*, 2019, **7(3):** 306–311.

[24] RÖMER H, LUTHER K D, ASSMUS W. Coloured zirconia. *Cryst. Res. Technol.*, 1994, **29(6):** 787–794.

[25] LV H D, BAO J X, CHAO L M, *et al*. Development mechanism of Ce-doped red zirconia ceramics prepared by a high-temperature reduction method. *J. Alloys Compd.*, 2019, **797:** 931–939.

[26] LEE D Y, KIM D J, SONG Y S. Chromaticity, hydrothermal stability, and mechanical properties of t-ZrO_2/Al_2O_3 composites doped with yttrium, niobium, and ferric oxides. *J. Mater. Sci. Eng. A*, 2000, **289(1/2):** 1–7.

[27] HOLZA L, MACIASB J, VITORINOB N, *et al*. Effect of Fe_2O_3 doping on colour and mechanical properties of Y-TZP ceramics. *Ceram. Int.*, 2018, **44(15):** 17962–17971.

[28] JOVANÍ M, FORTUÑO-MORTE M, BELTRÁN-MIR H, *et al*. Environmental-friendly red-orange ceramic pigment based on Pr and Fe co-doped $Y_2Zr_2O_7$. *J. Eur. Ceram. Soc.*, 2018, **38(4):** 2210–2217.

[29] WILLEMS E, ZHANG F, VAN MEERBEEK B, *et al*. Iron oxide colouring of highly-translucent 3Y-TZP ceramics for dental restorations. *J. Eur. Ceram. Soc.*, 2019, **39(2/3):** 499–507.

[30] SALEHI S, FATHI M H. Fabrication and characterization of Sol-Gel derived hydroxyapatite/zirconia composite nanopowders with various yttria contents. *Ceram. Int.*, 2010, **36(5):** 1659–1667.

[31] SU S, LIU Q, HU Z W, *et al*. A simple way to prepare Co:$MgAl_2O_4$ transparent ceramics for saturable absorber. *J. Alloys Compd.*, 2019, **797:** 1288–1294.

[32] CHEN P H, LIU Q, FENG Y G, *et al*. Transparent $Y_{0.16}Zr_{0.84}O_{1.92}$ ceramics sintered from co-precipitated nanopowder. *Opt. Mater.*, 2020, **100:** 109645–1–6.

[33] NIKL M, LAGUTA V V, VEDDA A. Complex oxide scintillators: material defects and scintillation performance. *Phys. Stat. Sol.*, 2008, **245(9):** 1701–1722.

两步烧结法制备红色 Ce:8YSZ 透明陶瓷及其性能研究

刘　强[1], 王　倩[1,2], 陈鹏辉[2,3], 李晓英[2,3], 章立轩[2,3], 谢腾飞[2,3], 李　江[2,3]

(1. 江苏大学 材料科学与工程学院, 镇江 212013; 2. 中国科学院 上海硅酸盐研究所, 透明光功能无机材料重点实验室, 上海 201899; 3. 中国科学院大学 材料科学与光电工程中心, 北京 100049)

摘　要: 彩色氧化锆陶瓷具有鲜艳色彩、高折射率、耐磨损、耐腐蚀及对人体无毒等优点, 被广泛应用于电子、装饰等领域。本研究采用共沉淀法合成了平均粒径为 15.9 nm 的立方相 Ce:8YSZ 纳米粉体。以经过 800 ℃煅烧 4 h 的粉体为原料, 通过两步烧结技术制备了具有高光学透过率和高红色度的 Ce:8YSZ 透明陶瓷，并系统研究了空气预烧温度对红色 Ce:8YSZ 透明陶瓷微观结构、直线透过率和色度的影响。当预烧温度从 1200 ℃升高到 1300 ℃时, Ce:8YSZ 陶瓷的平均晶粒尺寸从 0.3 μm 增大到 2.2 μm, 同时相对密度从 87.2%增加到 97.1%。经过 1275 ℃空气预烧 2 h 并结合 1700 ℃热等静压烧结 3 h 所得的 Ce:8YSZ 透明陶瓷表现出最佳的光学质量和最大的红色度值, 在 700 nm 处的直线透过率为 47.6%, 红色度为 52.0。

关　键　词: Ce:8YSZ; 红色透明陶瓷; 空气预烧; 热等静压烧结; 光学性能

中图分类号: TQ174　　**文献标志码**: A

我与郭景坤先生

2000 年 7 月, 我大学毕业到中国科学院上海硅酸盐研究所潘裕柏老师课题组工作。当时我的办公室正好在郭先生办公室隔壁, 让我有很多机会与先生近距离接触。郭先生给人的印象是平易近人、知识渊博、科研功底深厚。受郭先生的感染, 我入所没多久就立志要攻读研究生。经过努力, 我顺利通过国家研究生入学考试, 并幸运地成为郭先生和潘老师的研究生。2002 年 9 月, 我进入中国科学技术大学联合培养, 也是在这一年郭先生发现自己的声音变得嘶哑。2003 年 6 月底, 我回到所里开展“稀土离子掺杂 YAG 激光透明陶瓷的制备、结构及性能研究”的课题研究。同年 8 月, 郭先生查出来患了喉癌, 他用自己的嗓音在我主持的“青年学术沙龙”上做了最后一次学术报告“碳纤维补强石英复合材料及其应用”。2003 年 9 月, 郭先生进行了全喉切除手术, 从此他再也无法正常发音了。癌症手术后的生活中, 郭先生把更多的精力放在研究生的培养与指导上, 他借助人工发声装置经常跟我讨论研究课题, 并提出解决问题的建议, 帮助我成功研制出高性能的 YAG 激光陶瓷。研究生期间我撰写的每一篇学术论文, 郭先生都一字一句仔细修改, 使我的科研论文撰写能力得到不断提升。在与癌症抗争期间, 郭先生表现出来的积极乐观深深地鼓舞了我, 让我在科研生活中遇到任何困难都不会轻言放弃。这些年来, 郭先生主张逆向思维, 提倡标新立异, 追求事物本质的科学精神也一直激励着我。我希望自己能像郭先生一样, 在自己的研究领域挥洒汗水与智慧, 在科研的道路上发光发热。

左二: 李　江; 左四: 郭景坤先生

(李　江)